

Orbital Signatures of Methyl in L-Alanine

Chantal T. Falzon,[†] Feng Wang,^{*,‡} and Wenning Pang[‡]*Centre for Molecular Simulation, Swinburne University of Technology, P.O. Box 218, Hawthorn, Melbourne, Victoria 3122, Australia, and Polarization Physics Laboratory, Department of Physics, Tsinghua University, Beijing 100084, China**Received: February 7, 2006; In Final Form: March 19, 2006*

Molecular orbital signatures of the methyl substituent in L-alanine have been identified with respect to those of glycine from information obtained in coordinate and momentum space, using dual space analysis. Electronic structural information in coordinate space is obtained using *ab initio* (MP2/TZVP) and density functional theory (B3LYP/TZVP) methods, from which the Dyson orbitals are simulated based on the plane wave impulse approximation into momentum space. In comparison to glycine, relaxation in geometry and valence orbitals in L-alanine is found as a result of the attachment of the methyl group. Five orbitals rather than four orbitals are identified as methyl signatures. That is, orbital 6a in the core shell, orbitals 11a and 12a in the inner valence shell, and orbitals 19a and 20a in the outer valence shell. In the inner valence shell, the attachment of methyl to glycine causes a splitting of its orbital 10a' into orbitals 11a and 12a of L-alanine, whereas in the outer valence shell the methyl group results in an insertion of an additional orbital pair of 19a and 20a. The frontier molecular orbitals, 24a and 23a, are found without any significant role in the methylation of glycine.

1. Introduction

The dynamic roles of α -amino acids ($\text{NH}_2\text{—CH(R)—COOH}$) as building blocks of proteins rely heavily on their torsional flexibility, their unique shape, and chemical versatility of their side chains (R). Spatial and biochemical properties of proteins are dictated by these properties and consequently have significant ramifications in cellular processes, three-dimensional folding, and protein stability.¹ For this reason, understanding the dynamics of proteins through analysis of the structural and chemical properties of amino acids, in particular their side chains, under isolated conditions is of great importance.

With respect to molecular structure, the smallest chiral amino acid is L-alanine ($\text{R} = \text{CH}_3$). Alanine is a nonessential amino acid that is involved in the metabolism of tryptophan and the vitamin pyridoxine. It is an amino acid widely used in protein construction, averaging about 9% of protein composition on a per-mole basis when compared to other amino acids.² Experimental studies involving gas-phase electron diffraction (GED) techniques³ and the millimeter wave (MMW) spectrum of alanine⁴ indicate that isolated alanine exists in the molecular form and adopts several conformations; up to 13 possible conformations were predicted from sophisticated *ab initio* calculations.^{5–8} The relative stability and behavior of these conformers depend on the interplay of various intramolecular hydrogen bonds and electron correlation, which has been demonstrated for small aliphatic amino acids including glycine,^{9–15} alanine,^{4,16} and valine.¹⁷ The lowest-energy configuration of L-alanine is stabilized by an intramolecular hydrogen bond from the amine to the carbonyl ($\text{N—H}\cdots\text{O=C}$) and an interaction within the *cis* carboxylic functional group (Figure 1). The attachment of methyl with respect to glycine complicates the conformational landscape of L-alanine, which gives rise to the

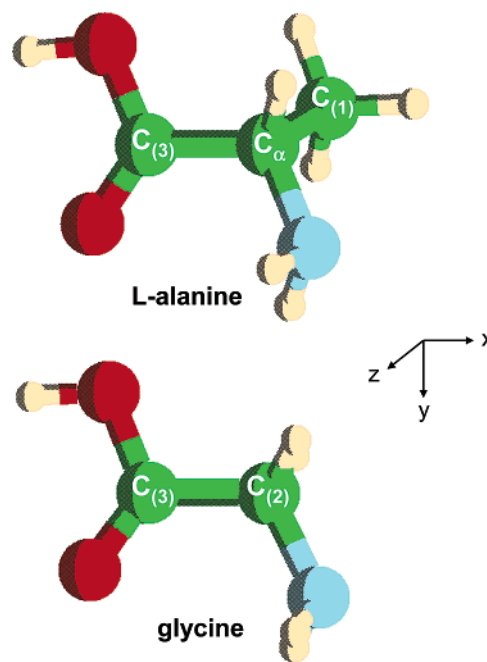


Figure 1. Chemical structures and numbering system of L-alanine and glycine.

increased number of plausible conformations. Nonetheless, limited information regarding the effects caused by inclusion of the methyl substituent exists in the literature. In the GED studies, Iijima and Beagley³ indicated that “the methyl group hinders rotation of the acid group” as the result of strong repulsion between the methyl and the hydroxy groups.

In a previous communication we provided an orbital-based insight into the bonding environment within the conformational processes of L-alanine, using both density functional theory (DFT) and *ab initio* methods.¹⁸ We focused on information that differentiated the conformers, such as dipole moments and

* Author to whom correspondence should be addressed. E-mail: fwang@swin.edu.au.

[†] Swinburne University of Technology.

[‡] Tsinghua University.

TABLE 1: Geometries of the Global Minimum Conformations of L-Alanine and Glycine Obtained Using the B3LYP/TZVP Model and Compared with Results Taken from the Literature

parameter	alanine				glycine ^a
	B3LYP/TZVP ^b	MP2/TZVP ^c	Császár ^d	expt ^e	
C ₍₃₎ =O/Å	1.211	1.211	1.211	1.197 ^f	1.204
C ₍₃₎ -O/Å	1.360	1.360	1.356	1.341 ^f	1.354
O-H/Å	0.972	0.972	0.968	0.977	0.969
C ₍₃₎ -C _α /Å	1.528	1.528	1.521	1.527 ^f	1.524
C ₍₁₎ -C _α /Å	1.537	1.537	1.530	1.536 ^f	
C _α -N/Å	1.457	1.457	1.452	1.453	1.451
C _α -H/Å	1.093	1.094	1.092		1.081
N-H/Å	1.016	1.016	1.016		1.001
H-O-C ₍₃₎ /deg	107.0	107.0	106.2	112.3	106.9
O=C ₍₃₎ -C _α /deg	125.6	125.5	125.4	125.7 ^f	124.5
O-C ₍₃₎ -C _α /deg	112.0	112.0	111.4	110.3	111.5
C ₍₃₎ -C _α -R/deg	109.2	109.2	108.3	111.9 ^f	107.5
C ₍₃₎ -C _α -N/deg	113.5	113.5	113.7	112.9 ^f	115.5
H-O-C ₍₃₎ -C _α /deg	178.2	178.2	176.9	180.0	180.0
O=C ₍₃₎ -C _α -N/deg	-19.7	-19.7	-20.5	-16.6 ^f	0.0
O-C ₍₃₎ -C _α -N/deg	161.1	161.0	161.3	162.8	180.0
C ₍₃₎ -C _α -N-H/deg	55.8	55.8	57.8		58.4
C ₍₃₎ -C _α -N-H/deg	-60.8	-60.8	-58.4		-58.4
O-C ₍₃₎ -C _α -H/deg	41.5	41.5			56.6
O-C ₍₃₎ -C _α -R/deg	-75.5	-75.4	-76.6		
<i>E</i> _{(total)/E_h}	-323.86402	-322.94026	(-323.85603) ^g		-284.536044
Dipole Moment					
μ _x /D	0.72 (0.62) ^c		0.60 ^h	0.66 ^j	-0.82 (-1.03) ^c
μ _y /D	0.98 (1.19) ^c		1.20 ^h	1.60 ^j	0.86 (0.82) ^c
μ _z /D	-0.46 (-0.48) ^c		0.50 ^h	0.40 ^j	0.00
μ/D	1.30 (1.43) ^c		1.40 ^h (1.41) ⁱ	1.8 ^j	1.19 (1.31) ^c

^a C₍₂₎ in glycine corresponds to the C_α atom in L-alanine; see ref 15. ^b This work. ^c The MP2/TZVP model used in the present study. ^d The MP2/6-311++G(d,p), ref 8. ^e Reference 3. ^f Electron diffraction, ref 42. ^g The B3LYP/6-311++G(d,p) model, ref 8. ^h The RHF/6-311++G(d,p) model, ref 8. ⁱ The MP2/6-311++G(d,p) model, ref 16. ^j Reference 4.

orbital momentum distributions (MDs), using dual space analysis (DSA).¹⁹ In this paper, we focus on the effects of substitution of methyl in glycine to the bonding environment in both position and momentum space, using DSA. We utilize anisotropic properties of L-alanine, such as dipole moments, Dyson orbitals, and their momentum distributions. For this purpose we investigated the lowest-lying-energy conformation of L-alanine using ab initio (MP2) and DFT B3LYP methods, in comparison with glycine.

2. Methods and Computational Details

Ground-state geometry calculations for L-alanine (C₁) were performed using the ab initio (MP2) and density functional theory (DFT) B3LYP methodology, together with the triple-ζ valence polarized (TZVP) basis set of Godbout et al.²⁰ The B3LYP/TZVP model has proved reliable in providing accurate information not only in properties but also in orbital momentum distributions for molecular systems,^{15,19,21–26} which were examined using electron momentum spectroscopy (EMS).²⁷ All electronic calculations undertaken in this investigation used the computational chemistry package of Gaussian 03.²⁸ The same procedure was applied to glycine for comparison purposes.

To generate accurate wave functions at the optimized geometry, due to technical reasons,¹⁹ additional single-point calculations (B3LYP/TZVP//B3LYP/TZVP) of L-alanine were undertaken. Under the Born–Oppenheimer approximation, independent particle approximation, and the plane wave impulse approximation (PWIA),²⁷ these wave functions were then Fourier-transformed into **k**-space as momentum distributions (MDs, σ)

$$\sigma \propto \int d\Omega |\psi_j(\mathbf{k})|^2$$

which is proportional to the momentum space one-electron Dyson orbitals $\psi_j(\mathbf{k})$. Dyson orbitals represent the changes in electronic structure accompanying the detachment of an electron from a molecule.²⁹ Corresponding to each ionization energy in the DFT calculations, the Dyson orbitals are proportional to canonical Kohn–Sham (KS) orbitals.³⁰ This method is implemented in the AMOLD codes.²⁷ For sufficiently high impact energies,³¹ the PWIA is a good approximation for valence orbitals³² in ground electronic states of molecules,³³ as confirmed by the EMS measurement for NNO.³⁴

3. Results and Discussion

3.1. Properties of L-Alanine. Figure 1 depicts the lowest-energy conformations of glycine¹⁵ (−284.5360437 *E_h*, B3LYP/TZVP) and L-alanine (−323.864023 *E_h*), which have been identified by previous experimental and theoretical calculations.^{4–8,16} Optimized geometric parameters for these conformers, including energetic information, are presented in Table 1. The predicted properties of L-alanine in the present study agreed satisfactorily with both experimental results and previous theoretical predictions.⁸ Bond distances for all characteristic single bonds (C_α–N, C₍₃₎–O, C_α–C₍₁₎) exhibit only minor variations with less than 0.02 Å from the experimental values. Bond angles and dihedral angles show larger deviations between the predicted and the measured.³⁵ For example, for the $\angle\text{HOC}_{(3)}$ angle, the largest discrepancy between the present method and the measured value is 5.3°, whereas the discrepancy of this angle produced using the MP2/6-311++G** method⁸ and the experiment is 6.0°. However, bond angles are, in general, less sensitive to energy variations so that they are more difficult to predict in quantum mechanics.

Structural relaxation in L-alanine directly associated with the methyl group with respect to glycine is also evident in Table 1.

The most significant geometrical changes in L-alanine with respect to the methyl attachment are the out-of-plane changes to the backbone atoms. In glycine, all of the backbone (non-hydrogen) atoms are confined in the same plane, and the $-\text{CH}_2$ and $-\text{NH}_2$ groups are symmetric with respect to the molecular plane. When one of the hydrogen atoms in the $-\text{CH}_2$ group is replaced by methyl (CH_3), the C_s symmetry is broken as the dihedral angle formed by planes consisting of $\text{O}=\text{C}_{(3)}-\text{O}$ and $\text{C}_{(3)}-\text{C}_\alpha-\text{N}$ changes from 0° in glycine to approximately 20° in L-alanine. The next significant change is the 15° distortion to the $\text{O}=\text{C}_{(3)}-\text{C}_\alpha-\text{H}$ dihedral angle, which indicates the degree of asymmetry caused by the $-\text{C}_\alpha\text{H}(\text{CH}_3)$ fragment in L-alanine. Comparison of the geometric parameters in L-alanine and glycine indicates that relaxation of varying degrees occurs to accommodate the methyl group. Relative to the values based on the B3LYP/TZVP model, a few characteristic differences are especially pronounced. For example, decreases of 2° of $\text{C}_{(3)}-\text{C}_\alpha-\text{N}$ and 1.7° of $\text{C}_{(3)}-\text{C}_\alpha-\text{R}$ ($\text{R} = \text{H}$ or CH_3), respectively, are observed in L-alanine. This is consistent with the findings of Császár⁸ who showed that a $2-3^\circ$ reduction occurs in this region using the MP2/6-311++G** method.

Analysis of dipole moments serves as a reference for monitoring the impact of the methyl group ($\text{R} = \text{CH}_3$) on polarity in L-alanine. The total dipole moment increases from 1.31 D in glycine to 1.43 D in L-alanine upon methylation, according to our MP2/TZVP method (Table 1). These values agree satisfactory with the experimental dipole moments of 1.0–1.4³⁶ and 1.8 D⁴ and the predicted dipole moments of 1.2 and 1.4 D¹⁶ using the MP2/6-311++G** model. The redistribution of charge becomes more indicative upon inspection of the individual dipole moment components. The μ_x component in glycine is -1.03 D and significantly changes to 0.62 D in L-alanine, whereas μ_y varies slightly, without any changes of sign. The nonzero μ_z component in L-alanine is purely from the charge redistribution caused by methylation in relation to the nonplanarity of the backbone atoms in L-alanine. The dipole moment in glycine (see Figure 1) is dominated by the amine group $-\text{NH}_2$, as the O pair is balanced out in the $+y$ and $-y$ directions. When a hydrogen on the C_α site is replaced by methyl, $-\text{CH}_3$, which acts as an electron acceptor, the charge distribution of L-alanine is thus significantly different in the x and z directions so that μ_x and μ_z are significantly varied.

3.2. Molecular Orbital Information in Coordinate Space.

In their ground electronic states, L-alanine (X^1A) and glycine (X^1A') both have closed shells with singlet states, with 24 and 20 doubly occupied molecular orbitals (MOs), respectively. The methyl group brings an additional eight electrons, which ought to form four doubly occupied MOs in L-alanine, one in the core and three in the valence regions. Table 2 lists the orbital energies of the core, inner, and outer valence shells of the amino acid pair. Methylation of glycine in the core shell is readily identified as MO 6a ($\text{C}_{(1)}$), as the core orbitals are localized on the individual atom sites. However, while methylation causes only small variations in energy to the core shell, it is interesting that the core orbital energies of all atom sites shift up (less negative) except for the C_α site, which shifts down in energy.

Relative to glycine, the orbitals in valence space (inner and outer) of L-alanine consist of three catalogues, methyl-dominated signature orbitals, methyl-affected (associated) orbitals, and methyl-perturbed orbitals, as indicated in Figure 2. The methyl-dominated orbitals of 11a, 12a, 19a, and 20a are direct contributions from methyl, which are signature orbitals of methyl. The methyl-affected (associated) orbitals are those with apparent energy shift in the immediate vicinity of the signature

TABLE 2: Orbital Energies ($-\epsilon_i$) and Symmetry Labels of L-Alanine Calculated Using the B3LYP/TZVP//B3LYP/TZVP Model, with Reference to Glycine

alanine (X^1A)				glycine (X^1A')			
MO	$-\epsilon_i/\text{eV}$	symmetry	site	MO	$-\epsilon_i/\text{eV}$	symmetry	site
core							
1	522.177	1a	O_H	1	522.218	1a'	O_H
2	520.651	2a	$\text{O}=\text{C}$	2	520.708	2a'	$\text{O}=\text{C}$
3	389.375	3a	N	3	389.479	3a'	N
4	280.775	4a	$\text{C}_{(3)}$	4	280.869	4a'	$\text{C}_{(3)}$
5	278.377	5a	C_α	5	278.276	5a'	C_α
6	276.973	6a	$\text{C}_{(1)}$				
inner valence							
7	30.477	7a		6	30.527	6a'	
8	28.084	8a		7	28.151	7a'	
9	24.577	9a		8	24.525	8a'	
10	20.766	10a		9	19.968	9a'	
11	18.445	11a		10	16.779	10a'	
12	16.269	12a					
outer valence							
13	14.346	13a		11	14.208	1a''	
14	13.685	14a		12	13.990	11a'	
15	13.501	15a		13	13.600	12a'	
16	12.581	16a		14	12.497	2a''	
17	12.085	17a		15	12.059	13a'	
18	11.582	18a		16	11.325	14a'	
19	10.684	19a					
20	10.537	20a					
21	10.029	21a		17	10.515	3a''	
22	9.225	22a		18	9.298	4a''	
23	8.063	23a		19	8.196	15a'	
24	7.090	24a		20	7.148	16a'	

orbitals as shown in Figures 2a and 2b. That is 10a, 13a, and 14a orbitals in the inner valence shell and orbitals 18a and 21a in the outer valence shell. In the inner valence shell, the influence of methyl on orbitals 7a, 8a, and 9a is negligible, whereas the methyl-affected orbitals (10a, 13a, and 14a) span in both sides of the methyl signature orbitals of 11a and 12a, spreading into the outer valence shell (13a and 14a). The inner valence shell orbitals 7a, 8a, and 9a of L-alanine, which are located in a region sufficiently far from the methyl signature orbitals of 11a and 12a, receive only small energy perturbations, as shown in Figure 2a. Hence, orbitals 7a, 8a, and 9a of L-alanine are catalogued as methyl-perturbed orbitals. The methyl signature orbitals 11a and 12a in the inner valence shell are both correlated to orbital 10a' of glycine as indicated in Figure 2a. Further determination of the methyl signatures and the influence of methylation on its surrounding environment in this region require additional orbital-based information.

Even though significant electron charge density delocalization brings more difficulties in the identification of methyl orbitals, it is possible, in the inner valence shell, to distinguish the dominant contribution through orbital symmetry and analogy between L-alanine and glycine. Similar trends in the outer valence space are observed in Figure 2b; only the orbitals in the immediate vicinity of the methyl signature orbitals receive apparent relaxation to accommodate the insertion of the methyl orbitals. The influence of methyl on other orbitals dwindles as the orbitals leave the methyl region of 10–11 eV. The insertion of orbitals 19a and 20a causes the surrounding orbitals to contract upon the inclusion; the most affected outer valence orbitals in L-alanine by such an orbital insertion are 18a and 21a, which correlate with MOs 14a' and 3a'' in glycine, respectively. The energy shifts in the orbital pairs of 1a''(Gly)–13a'(Ala) and 11a'(Gly)–14a(Ala) have been considered in the inner valence shell, whereas the orbital pair of 18a and 21a, in L-alanine, are influenced by the methyl signature orbitals (19a

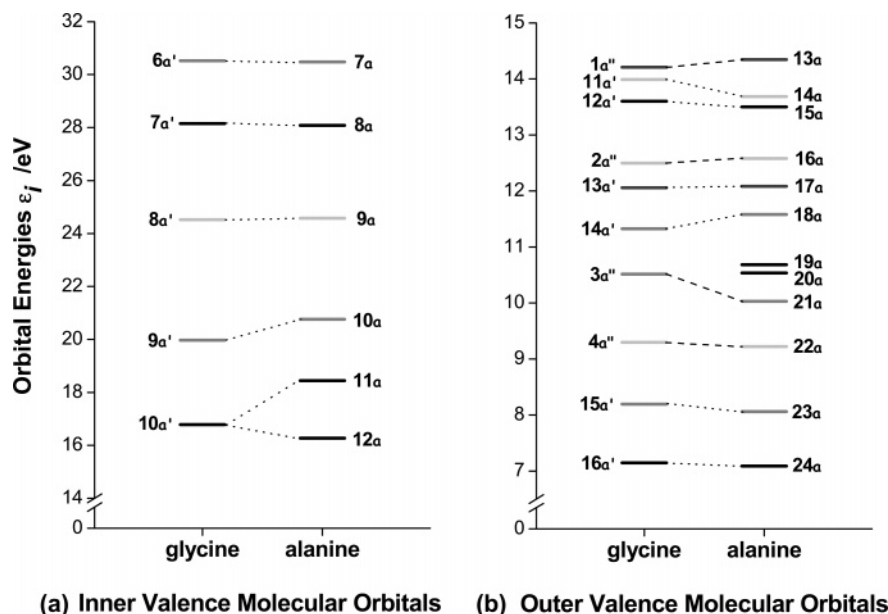


Figure 2. Orbital energy topology of complete valence shell of L-alanine, with respect to glycine calculated using the B3LYP/TZVP model.

and 20a) in the outer valence shell. Note that due to the lack of symmetry present in L-alanine and electron delocalization, there is no strictly “black and white” assignment of the L-alanine outer valence orbitals to the methyl group. Information regarding the domination of the methyl orbitals is further explored in the next section using information from momentum space.

3.3. Orbital MDs of L-Alanine in Valence Space. Orbital momentum distributions (MDs) in the complete valence space of L-alanine have been simulated in the present study. Although L-alanine lacks the symmetry present in glycine, we undertake correlation of two amino acids by comparison of symmetry, orbital energies, orbital electron densities, and Dyson orbital momentum distributions. Orbital MDs for glycine, which were simulated and examined previously¹⁵ using the same methodology, are employed as references to identify methylation in L-alanine. To simplify the analysis, the complete valence orbitals of L-alanine are discussed in groups: the methyl signature orbitals of 11a, 12a, 19a, and 20a; the methyl-affected orbitals of 10a, 13a, 14a, 18a, and 21a; and the perturbed orbitals consisting of the rest of valence orbitals including the highest occupied molecular orbital (HOMO), orbital 24a, and the next HOMO (NHOMO), i.e., orbital 23a. Figures 3–6 indicate the progressive changes in the valence orbitals of L-alanine with respect to glycine to reflect such grouping.

The methyl signature orbital MDs in the inner valence space (11a and 12a) of L-alanine are presented in Figure 3a, while Figure 3b gives orbital MDs of a methyl-affected orbital, 10a, with respect to glycine in the inner valence shell. The corresponding orbital contours plotted using Molden³⁷ are also given in these figures. In Figure 3a, orbitals 11a and 12a in L-alanine exhibit a unique relationship with orbital 10a' of glycine. The significant changes in the curvature of these orbital MDs indicate a large redistribution of electron density along the backbone of L-alanine, which is attributed to the methyl group. The orbital electron distribution highlights the enhancement of chemical bonding by the methyl. For example, orbital 11a(Ala) consolidates the bonding of C₃–C_α and the correlation between methyl and the amine group, whereas 12a(Ala) strengthens the correlation between the methyl group and the C–O(H) bond. However, the affected orbitals in the inner valence space, such as orbital 10a(Ala), in Figure 3b, which is correlated to orbital 9a' of glycine, reveals significant reduction in both s and p

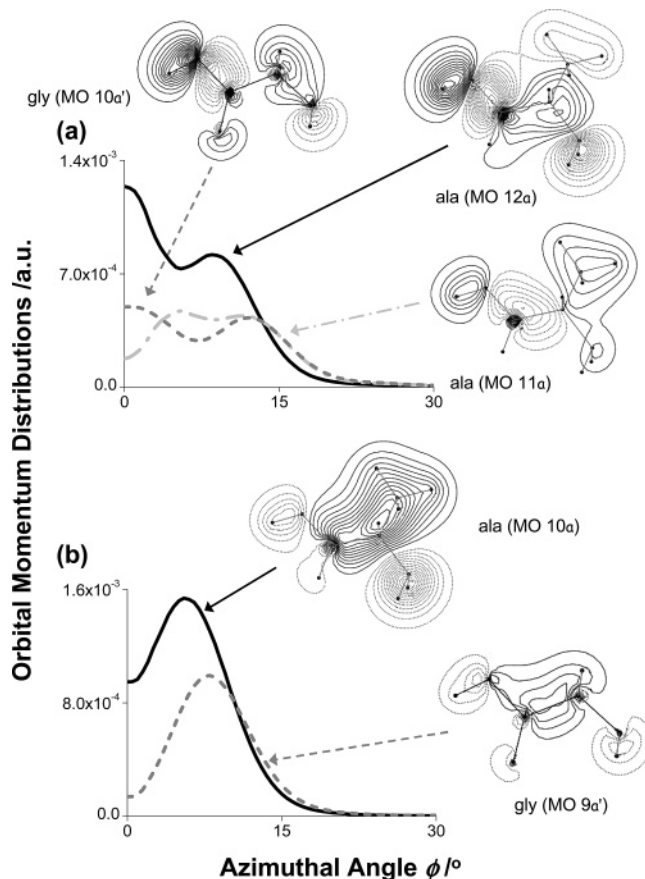


Figure 3. (a) Signature orbitals (11a and 12a) and (b) methyl-affected orbitals (10a) of L-alanine in the inner valence shell. The orbital electron densities are plotted using Molden.³⁷

contributions.¹⁵ The apparent s and p electron density enhancements of 10a (Ala) by methyl are particularly strong in the C₃–C_α–C₁ chain region.

Figure 4 gives the orbitals in the outer valence region of L-alanine that experience small perturbation by the methylation, such as the HOMO (24a), the next HOMO (23a), and the third HOMO (THOMO), orbital 22a. These frontier MOs have their own unique chemical significance, particularly in chemical

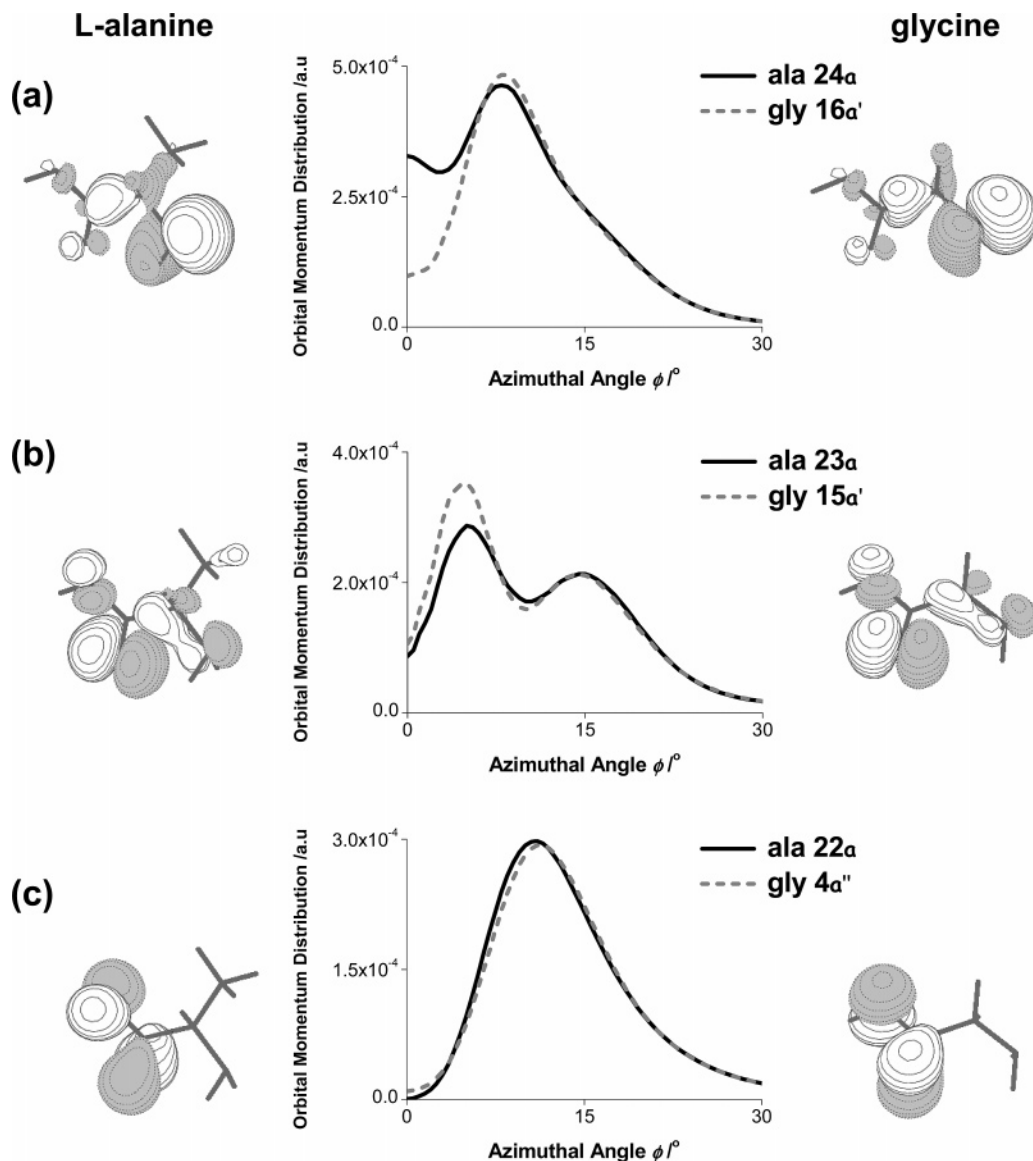


Figure 4. Selected orbitals (24a, 23a, and 22a) of the L-alanine least affected by the methyl in the outer valence shell: (a) orbital 24a (HOMO), which is dominated by N in the amine fragment, (b) orbital 23a (NHOMO), dominated by the O atom in the carboxylic C=O group, and (c) orbital 22a (THOMO), formed by the $2p_z$ orbitals of the pair of O atoms.

reactions involving structural manipulation. It is clear, however, that these orbitals are not too different from those of glycine upon the attachment of the methyl. For example, the orbital MDs for the HOMO of both glycine and L-alanine indicate mixed “s” and “p” features with a dominant “p-like” component, which stems from the large contributions made by the lone pair on the N atom of the amine group. The associated Dyson orbital contours also indicate an increase in s contributions in the C_α position across the molecular framework of $C_{(3)}-C_\alpha-N$ and $C_{(3)}-C_\alpha-CH_3$ upon methylation. The orbital MDs reflect this difference, particularly in the region of low momentum, demonstrating that orbital MDs can serve as a more sensitive and quantitative property in identifying electron redistribution than orbital contours. A similar trend is observed in the NHOMO of both species. Both NHOMOs in L-alanine and in glycine are dominated by the lone pair electrons on the O atoms of the acid functionality. The methyl group evidently has no active role in the outermost valence region of L-alanine as the interactions between the methyl and the glycine fragments exhibit very limited influence on the O and N dominant orbitals. This is further highlighted in the THOMO, orbital 22a of L-alanine, where the correlations between L-alanine and the

corresponding glycine orbital, MO 4a'', are almost undisturbed as demonstrated by their orbital MDs and orbital contours. This orbital pair, which concentrates on the $H-O-C_{(3)}=O$ fragment, is dominated by p electron contributions from the $2p_z$ atomic orbitals (AOs) of the carboxylic O and C atoms that form π -bonds perpendicular to the molecular plane (in glycine), indicating that the methyl does not actively participate in the local bonding of this region. The observation that frontier orbitals of molecules do not always exhibit an active role in reactions is supported by recent studies.^{38,39}

The methyl-affected orbitals in the outer valence shell of L-alanine provide insight into the localized changes with respect to glycine. As a representative for this group, orbital 21a of L-alanine and the respective orbital 3a''(Gly) is given in Figure 5. The orbital pair 21a(Ala)–3a''(Gly) correlates an a orbital (Ala) with an a'' orbital (Gly), the same symmetry correlation as the orbital pair of 22a(Ala)–4a''(Gly), as previously mentioned. However, the 21a(Ala)–3a''(Gly) pair is significantly different from the 22a(Ala)–4a''(Gly) pair in energy and Dyson orbitals. The orbital symmetry difference in the 22a(Ala)–4a''(Gly) pair is solely due to the absence of a molecule plane in L-alanine. The Dyson orbitals associated with this pair (Figure

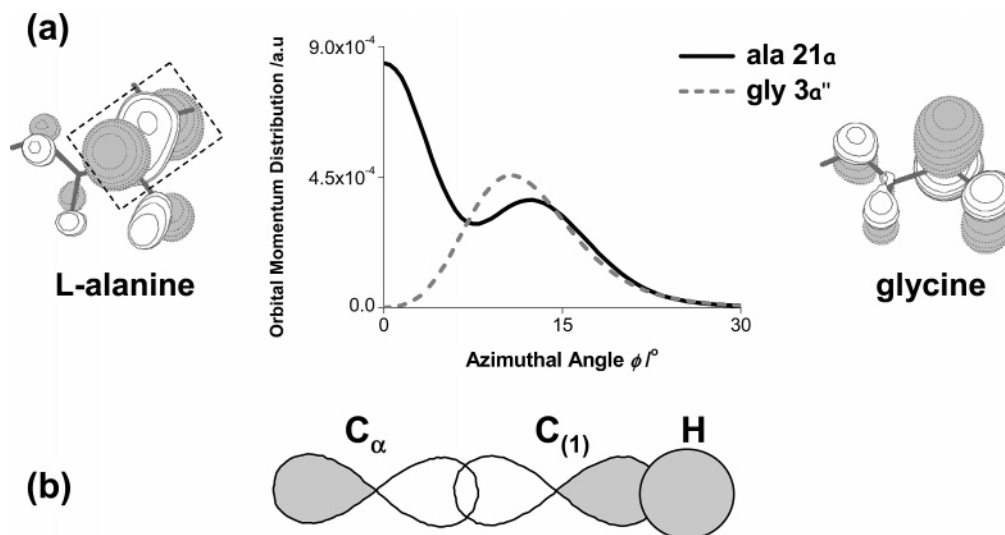


Figure 5. (a) Momentum and charge distributions of orbital 21a of L-alanine, as a representative of the methyl-affected orbitals in the outer valence shell. (b) Illustration of the $C_{\alpha}-C_{(1)}-H_{(\text{flag})}$ fragment bonding mechanism (boxed) in orbital 21a of L-alanine.

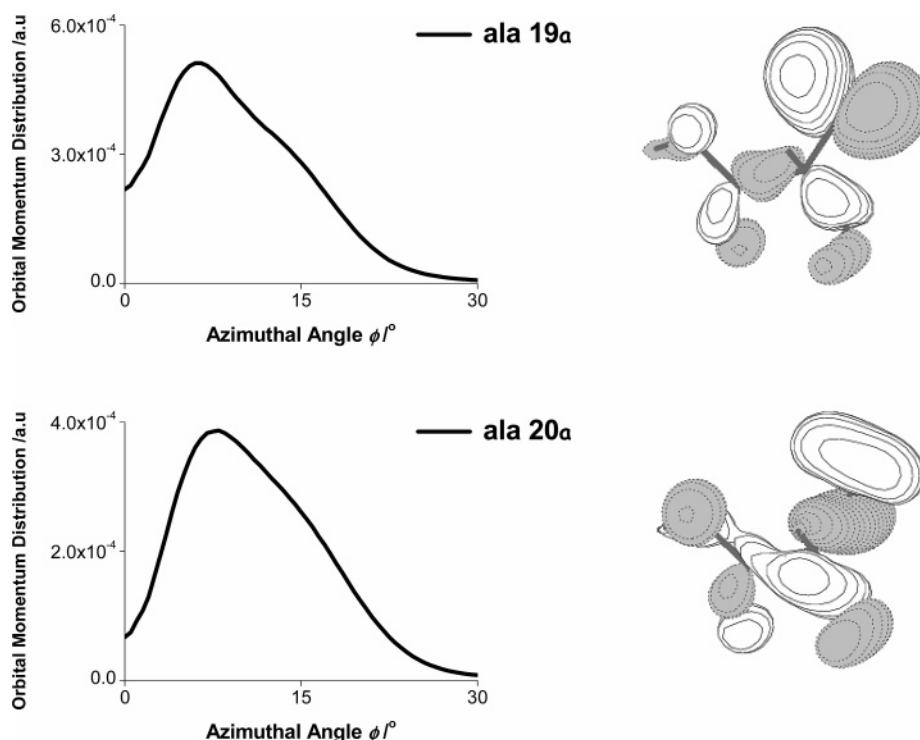


Figure 6. Momentum distributions and charge distributions of the methyl signature orbitals (19a and 20a) of L-alanine in the outer valence shell.

4c) reveal that they are in fact locally identical. In the 21a-(Ala)-3a''(Gly) pair, however, the differences between L-alanine and glycine are not just due to the symmetry but are also caused by the significant involvement of the methyl contribution to the orbital, as seen in Figure 5. In glycine, this orbital is dominated by contributions from the $C_{(2)}-H$ ($C_{(2)}$ in glycine is C_{α} in L-alanine) pair and the $N-H$ pair. In L-alanine, orbital 21a is dominated by the fragment of $C_{\alpha}-C_{(1)}-H$, as shown by the Dyson orbitals in Figure 5a. Upon methylation, the NH_2 contribution remains but with some distortion, whereas the symmetry of the $C_{\alpha}H_2$ fragment no longer exists; the $H-C_{\alpha}-H$ fragment is replaced by the $H-C_{\alpha}-C_{(1)}H_3$ fragment. Hence the two $2p_z$ AOs of C_{α} and $C_{(1)}$ each bond in a σ -like fashion. The outer side of the $2p_z$ AO of $C_{(1)}$ overlaps with the $1s$ AO of the flag H, which is the extension of $C_{(1)}-H$ in the methyl functionality in L-alanine, as indicated in the box in Figures 5a

and 5b. As a result, the orbital MDs of 21a(Ala) exhibit a significant s contribution, deviating from its glycine counterpart.

Figure 6 details the signature orbitals due to the insertion of the methyl group in the outer valence region. Orbitals 19a and 20a of L-alanine do not have any recognizable glycine orbital analogy. The Dyson orbitals reveal that a significant proportion of the electron density is concentrated on the C_{α} atom of $C_{(3)}-C_{\alpha}$ and the methyl group, which indicates that the methyl group acts as an electron donor. This observation supports a previous finding that when bonded to unsaturated fragments methyl groups act as electron donors.^{40,41} The MDs of the methyl signature orbital pair indicate a strong p-like nature, which is clearly visible in the Dyson orbitals. In orbital 19a, the 2p AO contribution occurs from the lone pair on the O atom in $O=C_{(3)}$, the 2p contributions of the O and $C_{(3)}$ atoms in the $1s-(H)-(2p)O-(2p)C_{(3)}$ chain, the $2p(C_{\alpha})-2p(N)$, and the domi-

nant contribution from $2p(C_{\alpha})-2p_y(C_{(1)})-1s(H)$ (two Hs). In orbital 20a, the Dyson orbital is more delocalized than in orbital 19a, so that the contributions from the 1s AOs of the hydrogen atoms in orbital 20a do not show as strong s-like MDs as orbital 19a.

4. Conclusion

The orbitals of L-alanine in its ground electronic state ($X'A'$) exhibit shift and variations from those of glycine (X^1A') in both binding energy spectra and orbital momentum distributions. Five identified methyl signature orbitals of 6a ($C_{(1)}$), 11a, 12a, 19a, and 20a distribute in all regions of the electronic spectrum of the molecule, including the core (6a), inner valence shell (11a, 12a), and outer valence shell (19a, 20a). Although the core region of L-alanine exhibits negligible energy perturbations to other core orbitals, it is noted that the methyl fragment shifts all core orbitals energies up (less negative) with respect to their glycine counterparts. The exception is for C_{α} , which shifts the energy in the opposite direction. Inner and outer valence regions receive local relaxation to accommodate the insertion of the methyl group, and such relaxation fades away apparently when the orbital moves away from signature orbitals. In the inner valence shell, the methyl causes a splitting of orbital 10a' of glycine into orbitals 11a and 12a of L-alanine, whereas in the outer valence shell, the methyl group causes an insertion of an additional orbital pair of 19a and 20a in L-alanine. As a result, the methyl group signature orbitals are five rather than four. The methyl-affected orbitals that locate within the intermediate vicinity of the signature orbitals receive important contributions from the methyl attachment, due to spatial and electronic reasons, characterized by the interaction along the $C_{(3)}-C_{\alpha}-C_{(1)}H_3$ chain. The methyl group evidently has no active role in the bonding of the least affected orbitals, including frontier orbitals such as the HOMO, NHOMO, and orbital 22a of L-alanine.

Acknowledgment. The authors thank the Vice Chancellor's Strategic Research Initiative Grant of the Swinburne University of Technology. F.W. and W.N.P. acknowledge an ARC International Linkage Award. The Australian Partnership for Advanced Computing is thanked for the use of the National Supercomputing Facilities. W.N.P. thanks Project No. 10574074, supported by the National Natural Science Foundation of China.

References and Notes

- (1) Baldwin, T.; Lapointe, M. In *The Chemistry of Amino Acids: The Biology Project*; 2003. http://www.biology.arizona.edu/biochemistry/problem_sets/aa/aa.html.
- (2) Davidson, M. W. *Molecular Expressions: The Amino Acid Collection: Alanine*; 1995–2005. <http://micro.magnet.fsu.edu/aminoacids/pages/alanine.html>.
- (3) Iijima, K.; Beagley, B. J. *Mol. Struct.* **1991**, *248*, 133.
- (4) Godfrey, P. D.; Firth, S.; Hatherley, L. D.; Brown, R. D.; Pierlot, A. P. *J. Am. Chem. Soc.* **1993**, *115*, 9687.
- (5) Cao, M.; Newton, S. Q.; Pranata, J.; Schäfer, L. *J. Mol. Struct.: THEOCHEM* **1995**, *332*, 251.
- (6) Godfrey, P. D.; Brown, R. D.; Rodgers, F. M. *J. Mol. Struct.* **1996**, *376*, 65.
- (7) Kaschner, R.; Hohl, D. *J. Phys. Chem. A* **1998**, *102*, 5111.
- (8) Császár, A. G. *J. Phys. Chem.* **1996**, *100*, 3541.
- (9) Suenram, R. D.; Lovas, F. J. *J. Mol. Spectrosc.* **1978**, *72*, 372.
- (10) Suenram, R. D.; Lovas, F. J. *J. Am. Chem. Soc.* **1980**, *102*, 7180.
- (11) Lovas, F. J.; Kawashima, Y.; Grabow, J.-U.; Suenram, R. D.; Fraser, G. T.; Hirota, E. *Astrophys. J.* **1995**, *455*, L201.
- (12) Brown, R. D.; Godfrey, P. D.; Storey, J. W. V.; Bassez, M.-P. *J. Chem. Soc., Chem. Commun.* **1978**, 547.
- (13) Godfrey, P. D.; Brown, R. D. *J. Am. Chem. Soc.* **1995**, *117*, 2019.
- (14) McGlone, S. J.; Elmes, P. S.; Brown, R. D.; Godfrey, P. D. *J. Mol. Struct.* **1999**, *485*, 225.
- (15) Falzon, C. T.; Wang, F. *J. Chem. Phys.* **2005**, *123*, 214307.
- (16) Blanco, S.; Lesarri, A.; López, J. C.; Alonso, J. L. *J. Am. Chem. Soc.* **2004**, *126*, 11675.
- (17) Lesarri, A.; Cocinero, E. J.; López, J. C.; Alonso, J. L. *Angew. Chem., Int. Ed.* **2004**, *43*, 605.
- (18) Falzon, C. T.; Wang, F. In *Conformational Processes in L-Alanine Studied Using Dual Space Analysis*, Proceedings of the International Conference on Computational Science (ICCS 2006); Alexandrov, V. N., et al., Eds.; *Lecture Notes in Computer Science* 3993, Part III; Springer-Verlag: Berlin Heidelberg, 2006; pp 82–88.
- (19) Wang, F. *J. Phys. Chem. A* **2003**, *107*, 10199.
- (20) Godbout, N.; Salahub, D. R.; Andzelm, J.; Wimmer, E. *Can. J. Chem.* **1992**, *70*, 560.
- (21) Saha, S.; Wang, F.; Falzon, C. T.; Brunger, M. J. *J. Chem. Phys.* **2005**, *123*, 124315.
- (22) Wang, F.; Downton, M. T.; Kidwani, N. J. *Theor. Comput. Chem.* **2005**, *4*, 247.
- (23) Wang, F. *J. Mol. Struct.: THEOCHEM* **2005**, *728*, 31.
- (24) Wang, F.; Downton, M. *J. Phys. B: At. Mol. Opt. Phys.* **2004**, *37*, 557.
- (25) Downton, M.; Wang, F. *Chem. Phys. Lett.* **2004**, *384*, 144.
- (26) Wang, F.; Brunger, M. J.; McCarthy, I. E.; Winkler, D. A. *Chem. Phys. Lett.* **2003**, *382*, 217.
- (27) Weigold, E.; McCarthy, I. E. *Rep. Prog. Phys.* **1991**, *54*, 789.
- (28) Frisch, M. J.; Trucks, G. W.; Schlegel, H. B.; Scuseria, G. E.; Robb, M. A.; Cheeseman, J. R.; Montgomery, J. A., Jr.; Vreven, T.; Kudin, K. N.; Burant, J. C.; Millam, J. M.; Iyengar, S. S.; Tomasi, J.; Barone, V.; Mennucci, B.; Cossi, M.; Scalmani, G.; Rega, N.; Petersson, G. A.; Nakatsuji, H.; Hada, M.; Ehara, M.; Toyota, K.; Fukuda, R.; Hasegawa, J.; Ishida, M.; Nakajima, T.; Honda, Y.; Kitao, O.; Nakai, H.; Klene, M.; Li, X.; Knox, J. E.; Hratchian, H. P.; Cross, J. B.; Adamo, C.; Jaramillo, J.; Gomperts, R.; Stratmann, R. E.; Yazyev, O.; Austin, A. J.; Cammi, R.; Pomelli, C.; Ochterski, J. W.; Ayala, P. Y.; Morokuma, K.; Voth, G. A.; Salvador, P.; Dannenberg, J. J.; Zakrzewski, V. G.; Dapprich, A.; Daniels, A. D.; Strain, M. C.; Farkas, O.; Malick, D. K.; Rabuck, A. D.; Raghavachari, K.; Foresman, J. B.; Ortiz, J. V.; Cui, Q.; Baboul, A. G.; Clifford, S.; Cioslowski, J.; Stefanov, B. B.; Liu, G.; Liashenko, A.; Piskorz, P.; Komaromi, I.; Martin, R. L.; Fox, D. J.; Keith, T.; Al-Laham, M. A.; Peng, C. Y.; Nanayakkara, A.; Challacombe, M.; Gill, P. M. W.; Johnson, B.; Chen, W.; Wong, M. W.; Gonzalez, C.; Pople, J. A. *Gaussian 03*, revision C.02; Gaussian, Inc.: Wallingford, CT, 2004.
- (29) Dolgounitcheva, O.; Zakrzewski, V. G.; Ortiz, J. V. *J. Am. Chem. Soc.* **2000**, *122*, 12304.
- (30) Duffy, P.; Chong, D. P.; Casida, M. E.; Salahub, D. R. *Phys. Rev. A* **1994**, *50*, 4707.
- (31) Takahashi, M.; Saito, T.; Hiraka, J.; Udagawa, Y. *J. Phys. B: At. Mol. Opt. Phys.* **2003**, *36*, 2539.
- (32) Clark, S. A. C.; Reddish, T. J.; Brion, C. E.; Davidson, E. R.; Frey, F. R. *Chem. Phys.* **1990**, *143*, 1.
- (33) Takahashi, M.; Khajuria, K.; Udagawa, Y. *Phys. Rev. A* **2003**, *68*, 042710.
- (34) Khajuria, Y.; Takahashi, M.; Udagawa, Y. *J. Electron Spectrosc. Relat. Phenom.* **2003**, *133*, 113.
- (35) Oberhammer, H. *J. Comput. Chem.* **1998**, *19*, 123.
- (36) Suenram, R. D.; Lovas, F. J. *J. Am. Chem. Soc.* **1980**, *102*, 7180.
- (37) Schaftenaar, G.; Noordik, J. *J. Comput.-Aided Mol. Des.* **2000**, *14*, 123.
- (38) Jones, D.; Wang, F.; Brunger, M. J.; Winkler, D. A. *Biophys. Chem.* **2006**, *121*, 105.
- (39) da Silva, R. R.; Ramalho, T. C.; Santos, J. M.; Figueroa-Villar, J. D. *J. Phys. Chem. A* **2006**, *110*, 1031.
- (40) Sathre, L. J.; Berrah, N.; Bozek, J. D.; Børve, K. J.; Carroll, T. X.; Kukk, E.; Gard, G. L.; Winter, R.; Thomas, T. D. *J. Am. Chem. Soc.* **2001**, *123*, 10729.
- (41) Li, Q. Z.; Wu, G. S.; Yu, Z. W. *J. Am. Chem. Soc.* **2006**, *128*, 1438.
- (42) Iijima, K.; Nakano, M. *J. Mol. Struct.* **1999**, *485*, 255.